Journal of Cellular Biochemistry 104:162–175 (2008)

# *N*-Glycosylation Affects the Adhesive Function of E-Cadherin Through Modifying the Composition of Adherens Junctions (AJs) in Human Breast Carcinoma Cell Line MDA-MB-435

**Hongbo Zhao,[1,2] Yulong Liang,[1] Zhibin Xu,[1,2] Liying Wang,[1,2] Feng Zhou,[1,2] Zengxia Li,[1] Jiawei Jin,[1] Yong Yang,[1] Zhengyu Fang,[1] Yali Hu,[1] Lineng Zhang,[1] Jianmin Su,[1,2]* and Xiliang Zha[1,2]***

[1]Department of Biochemistry and Molecular Biology, Shanghai Medical College, Fudan University, 138 Yi Xue Yuan Road, Shanghai 200032, PR China
[2]Key Laboratory of Glycoconjugate Research, Ministry of Health, Shanghai Medical College, Fudan University, Shanghai 200032, PR China

**Abstract** E-cadherin mediates calcium-dependent cell–cell adhesion between epithelial cells. The ectodomain of human E-cadherin contains four potential *N*-glycosylation sites at Asn residues 554, 566, 618, and 633. In this study, the role of *N*-glycosylation in E-cadherin-mediated cell–cell adhesion was investigated by site-directed mutagenesis. In MDA-MB-435 cells, all four potential *N*-glycosylation sites of human E-cadherin were *N*-glycosylated. Removal of *N*-glycan at Asn-633 dramatically affected E-cadherin stability. In contrast, mutant E-cadherin lacking the other three *N*-glycans showed similar protein stability in comparison with wild-type E-cadherin. Moreover, *N*-glycans at Asn-554 and Asn-566 were found to affect E-cadherin-mediated calcium-dependent cell–cell adhesion, and removal of either of the two *N*-glycans caused a significant decrease in calcium-dependent cell–cell adhesion accompanied with elevated cell migration. Analysis of the composition of adherens junctions (AJs) revealed that removal of *N*-glycans on E-cadherin resulted in elevated tyrosine phosphorylation level of β-catenin and reduced β- and α-catenins at AJs. These findings demonstrate that *N*-glycosylation may affect the adhesive function of E-cadherin through modifying the composition of AJs. J. Cell. Biochem. 104: 162–175, 2008. © 2007 Wiley-Liss, Inc.

**Key words:** E-cadherin; *N*-glycosylation; cell–cell adhesion; β-catenin tyrosine phosphorylation; adherens junctions (AJs)

E-cadherin, an important member of the cadherin family, is usually expressed in epithelial cells and involved in calcium-dependent cell–cell adhesion. The highly conserved cytoplasmic domain of E-cadherin interacts with α-, β-, and γ-catenins, mediating connections between E-cadherin and the actin cytoskeleton [Provost and Rimm, 1999; Nagafuchi, 2001]. The ectodomain of E-cadherin contains five tandemly repeated extracellular domains (EC), each of which harbors ~110 amino acids and the first extracellular domain (EC1) governs the homophilic interactions of E-cadherin [Nose et al., 1990; Makagiansar et al., 2002]. As the key component of adherens junctions (AJs) in epithelial cells, E-cadherin participates in the maintenance of epithelial morphology and homoeostasis [Gottardi et al., 2001; Gumbiner, 2005; Tunggal et al., 2005].

The ectodomain of human E-cadherin contains four potential *N*-glycosylation sites at Asn residues 554, 566, 618, and 633 on the basis of amino acid sequence analysis (GenBank Accession L08599) [Rimm and Morpanels, 1994]. The

Grant sponsor: National Natural Science Foundation of China; Grant number: 30670468; Grant sponsor: Research Fund for Doctoral Program of Higher Education; Grant number: 20030246042; Grant sponsor: Foundation of Shanghai Municipal Health Bureau; Grant number: 044087.

Yulong Liang's present address is Department of Surgery, Baylor College of Medicine, Houston, TX 77030.

*Correspondence to: Jianmin Su and Xiliang Zha, Department of Biochemistry and Molecular Biology, Shanghai Medical College, Fudan University, 130 Dong An Road, Shanghai 200032, PR China.
E-mail: jimmysu1@yahoo.com; xlzha@shmu.edu.cn

Received 29 June 2007; Accepted 18 September 2007
DOI 10.1002/jcb.21608

© 2007 Wiley-Liss, Inc.

four *N*-glycosylation sites lie within the fourth and fifth extracellular domain of E-cadherin (EC4–EC5). Except that the *N*-glycosylation site at Asn-566 is unique to the human homolog of E-cadherin, the other three sites are conserved in human, mouse, and chicken E-cadherin [Kitada et al., 2001].

*N*-glycosylation is known to possess important functions for many proteins, as it affects protein stabilization, protein folding, quality control, endocytic sorting, and degradation [Rudd and Dwek, 1997; Helenius and Aebi, 2004]. To date, the structure and function of E-cadherin *N*-glycosylation remain elusive. Previously, structural modifications of E-cadherin *N*-glycosylation by *N*-acetylglucosaminyltransferase III (GnT III) were shown to cause increased cell–cell adhesion, whereas structural modifications of N-cadherin *N*-glycosylation by *N*-acetylglucosaminyltransferase V (GnT V) resulted in decreased cell–cell adhesion [Yoshimura et al., 1996; Kitada et al., 2001; Guo et al., 2003]. These observations indicated that *N*-glycosylation may affect cadherin-mediated cell–cell adhesion.

To systematically investigate the function of E-cadherin *N*-glycosylation, we obliterated each consensus sequence of human E-cadherin by substituting Gln for Asn, either individually or in combination, and expressed mutated cDNAs in human breast carcinoma MDA-MB-435 cells which lack E-cadherin expression at both the mRNA and protein levels. In the present study, we found that individual *N*-glycan of E-cadherin presents distinctive function. *N*-glycan at Asn-633, but not *N*-glycans at the other three sites, seems to be required for E-cadherin stability. However, *N*-glycans at Asn-554 and Asn-566 affect the adhesive function of E-cadherin significantly. Further studies revealed that *N*-glycosylation may affect the adhesive function of E-cadherin through modifying the composition of AJs.

## MATERIALS AND METHODS

### Plasmids Construction, Site-Directed Mutagenesis, and Transfections

The plasmid pcDNA3.0-Ecad containing human full-length E-cadherin cDNA was kindly supplied by Dr. Cara J. Gottardi (Memorial Sloan-Kettering Cancer Center, New York). To create either individual or combined mutations of *N*-glycosylation sites of E-cadherin, a PCR-based site-directed mutagenesis was carried out using a three-round method. In the first-round PCR, the forward primer was 5′-AGT GAC GAA TGT GGT ACC TTT TGA-3′ (for N554Q, N566Q, N618Q, and N633Q), and the reverse primers were 5′-TTA GGG CTG TGT ACG TGC TTT GCT TCA-3′ (for N554Q), 5′-AGC AAC TGG AGA ACC TTG GTC TGT AGC TAT-3′ (for N566Q), 5′-TGA AGG GAG ATG TTT GGG GAG GAA GGT C-3′ (for N618Q), and 5′-TAC TGA ATG GTC CATTGG GGC ACT CGC C-3′ (for N633Q). In the second round, the forward primers were 5′-TGA AGC AAA GCA CGT ACA CAG CCC TAA-3′ (for N554Q), 5′-ATA GCT ACA GAC CAA GGT TCT CCA GTT GCT-3′ (for N566Q), 5′-GAC CTT CCT CCC CAA ACA TCT CCC TTC A-3′ (for N618Q), 5′-GGC GAG TGC CCC AAT GGA CCA TTC AGT A-3′ (for N633Q), and the reverse primers were 5′-GC TCT AGA TCT CGA GTC CCC TAG TGG TCC-3′ (for N554Q, N566Q, N618Q, and N633Q). In the last round, PCR products from the first two steps were purified, ligated, and used to replace the similar fragment of human E-cadherin cDNA plasmid. Mutations were confirmed by automatic DNA sequencing wild-type and mutant E-cadherin cDNAs with one individual *N*-glycosylation site abrogated (M1-Ecad, N554Q; M2-Ecad, N566Q; M3-Ecad, N618Q; M4-Ecad, N633Q) and several *N*-glycosylation sites abrogated in combination (M123-Ecad, N554QN566QN618Q; M1234-Ecad, N554QN566QN618QN633Q) were purified and transfected into $3 \times 10^5$ MDA-MB-435 cells using Lipofectamine 2000 reagent (Invitrogen) according to the manufacturer's recommendations. Cell lines stably expressing wild-type or mutant E-cadherin cDNAs were selected by G418 (800 μg/ml) and screened by RT-PCR and Western blotting analysis.

### Cell Lines and Cell Culture

Human breast carcinoma cell line MDA-MB-435, mock (empty plasmid stably transfected MDA-MB-435), wtEcad-435 (wild-type E-cadherin stably transfected MDA-MB-435), M1-Ecad-435 (M1-Ecad stably transfected MDA-MB-435), M2-Ecad-435 (M2-Ecad stably transfected MDA-MB-435), M3-Ecad-435 (M3-Ecad stably transfected MDA-MB-435), M4-Ecad-435 (M4-Ecad stably transfected MDA-MB-435), M123-Ecad-435 (M123-Ecad stably transfected MDA-MB-435), and M1234-Ecad-435 (M1234-Ecad stably transfected

MDA-MB-435) cells were maintained in DMEM (Gibco, Invitrogen) supplemented with 10% fetal bovine serum (HyClone Laboratories) and 1% penicillin/streptomycin (Life Technologies, Inc).

### Reagents and Antibodies

Cycloheximide (CHX) was obtained from Amresco (Solon, OH). Tunicamycin (TM) was purchased from Sigma-Aldrich. Monoclonal antibodies to α-catenin, β-catenin, PY20, and tubulin were purchased from Santa Cruz. Monoclonal antibody to GAPDH and secondary antibodies conjugated with HRP were purchased from Kang-Chen Biotech (Shanghai, China).

### RT-PCR

Total RNAs were isolated using the Trizol system (Watson Biotechnologies, Shanghai, China) according to the manufacturer's guidelines. RT-PCR was performed to quantify the mRNA level of E-cadherin. Oligo dT primer and MMLV-RTase were used for first strand synthesis. cDNA products (2 μl) were mixed with Taq DNA polymerase (SABC, Luoyang, China), 50 pmol/L of each appropriate primer, 200 μmol/L each dNTP in a reaction buffer containing 10 mmol/L Tris–HCl (pH 8.3), 50 mmol/L KCl, 0.01% (W/V) bovine serum albumin (BSA), 2 mmol/L $MgCl_2$ in a final volume of 100 μl. The primer pair for E-cadherin was: 5′-AGT GAC GAA TGT GGT ACC TTT TGA-3′ (sense) and 5′-TAC TGA ATG GTC CAT TGG GGC ACT CGC C-3′ (anti-sense). The primer pair for β-actin was: 5′-TGG GCA TGG GTC AGA AGG AT-3′ (sense) and 5′-AAG CAT TTG CGG TGG ACG AT-3′ (anti-sense). The expected product sizes were as follows: E-cadherin, 507 bp; β-actin, 900 bp. The samples were amplified for 30 cycles at cyclic temperatures of 94°C 30 s, 56°C 30 s, 72°C 1 min. PCR products were analyzed through 1% agarose gel electrophoresis and following ethidium bromide staining. The band area of E-cadherin was measured and normalized by that of β-actin, and then the specific E-cadherin mRNA level was estimated.

### Western Blotting

Cells were lysed in 1 × SDS lysis buffer (50 mM Tris–HCl, pH 6.8, 2% SDS, 10% glycerol, 1 mM PMSF, and 1 mM $Na_3VO_4$) and performed as described previously [Liang et al., 2004]. Equal amount of total protein was loaded on an SDS–PAGE gel and transferred to PVDF membrane (Millipore). After blocked with 5% BSA in PBS (containing 0.05% Tween-20), the membrane was incubated with specific primary antibodies, and followed by incubation with HRP-conjugated secondary antibodies (Kang-Chen Biotech). Proteins were visualized by fluorography using an enhanced chemiluminescence system (Perfect Biotech, Shanghai, China).

### MALDI-TOF MS Analysis

E-cadherin mutant lacking *N*-glycans at Asn-554, Asn-566, and Asn-618 was purified by immunoprecipitation and analyzed on an 8% SDS–PAGE gel. The gel was stained with Coomassie blue and the protein band with expected size was excised and cut into small pieces. The Coomassie blue dye was removed by extraction of the gel with 50% acetonitrile. The gel was then dried and dissolved in 50 μl of ammonia bicarbonate buffer. Five units of PNGaseF (New England Biolabs, Inc., Ipswich, MA) were added in the buffer and incubated at 37°C for overnight. The released glycans were desalted by carbograph SPE column (Alltech Associates, Deerfield, IL). Bound glycans were eluted by 30% acetonitrile in 0.05% trifluoroacetic acid (TFA). The released clean glycans were labeled with 2-anthrailic acid (2-AA) and purified by paper disk [Xia et al., 2005]. The 2-AA labeled *N*-glycans were analyzed by matrix-assisted laser desorption/ionization time-of-flight mass spectrometry (MALDI-TOF MS), on Voyager-DE RP Biospectrometry Workstation instrument (Applied Biosystems, Framingham, MA). MALDI spectra were acquired at 25 kV accelerating voltage in negative mode and smoothed by applying a 19-point Savitzky–Golay smoothing routine. The 2,5-dihydroxybenzoic acid (DHB) was used as matrix and 10 mM ammonium citrate solution was added for depressing the salt ions. The instrument was calibrated with dextran ladder-2AA. Average masses of $[M-H]^-$ ions were calculated according to EXPASy GlycoMod Tool and Glycan Mass (http://us.expasy.org/tools/glycomod/).

### Cell Aggregation Assay

Cell aggregation assay was performed as described previously with minor modifications [Guo et al., 2003]. Cells were detached with HCMF buffer (150 mM NaCl, 0.6 mM $Na_2HPO_4$, 10 mM glucose and 10 mM HEPES, pH 7.4) containing 0.02% trypsin and 2 mM $CaCl_2$.

Single cell suspensions were re-suspended in HCMF buffer containing 2 mM $CaCl_2$ at a concentration of $10^5$ cells/ml. Aliquots of cell suspension (300 μl) were added to each well of 24-well plates pre-coated with 1% BSA and incubated for different times at 37°C with 80 rpm agitation. For some experiments, function blocking antibodies against N-cadherin (50 μg/ml, Santa Cruz), E-cadherin (DECMA, 1:100, Sigma), β1 integrin (50 μg/ml, Santa Cruz), α5 integrin (2 mg/ml, Santa Cruz), and nonimmune IgG (50 μg/ml, Santa Cruz) were added into the cell suspensions, respectively. The extent of cell–cell adhesion was represented by aggregation index (AI). AI was calculated as (No − Nt)/No, where No was the initial particle number before aggregation and Nt was the total particle number at a given time. Calcium-dependent aggregation was calculated by subtracting values obtained from aggregation assays in the presence of EGTA (2 mM) from the values of the total number of aggregating cells. The levels of aggregating cells in EGTA were typically <5% of the total number of aggregating cells.

### Cell Migration Assay

Cell migration was determined using transwell chamber assay as described previously with minor modifications [Bourguignon et al., 2000]. Cells were re-suspended in medium containing 0.1% BSA at a concentration of $10^6$ cells/ml and $2 \times 10^5$ cells were added to the top well of transwell chambers (Costar Corporation). The cell suspensions were then placed into the upper compartment and medium containing 5% fetal bovine serum were placed into the lower compartment as an inducer. After 12 h incubation, cells which had not migrated were removed from the upper face of the filters using cotton swabs, and cells which had migrated to the lower surface of the filters were fixed in methanol and stained by crystal violet. Migration was determined by counting the number of cells which had migrated to the lower surface. Six visual fields were counted for each essay.

### Preparation of Triton X-100-Insoluble Cytoskeletal Fractions

All procedures were performed as described previously [Kim et al., 2002]. Briefly, cells were lysed in a buffer containing 10 mM Tris–HCl, pH 6.8, 1 mM EDTA, 150 mM NaCl, 0.25% Nonidet P-40, 1% Triton X-100, 1 mM PMSF and 1 mM $Na_3VO_4$, and followed by centrifugation at 16,000*g*. For Triton X-100-insoluble cytoskeletal fractions, the remaining pellet was re-extracted twice with lysis buffer to ensure that all detergent-soluble material was removed. The final pellet after centrifugation at 16,000*g* was extracted with SDS-containing buffer (10 mM Tris–HCl, pH 6.8, 2 mM EDTA, 150 mM NaCl, 1% SDS). Equal amount of protein was loaded on a 10% SDS–PAGE gel, and then analyzed using Western blotting assay.

### Immunoprecipitation

Cells were washed three times with ice-cold PBS and solubilized with 1 ml lysis buffer (50 mM Tris–HCl, pH 7.5, 150 mM NaCl, 0.1% Nonidet P-40, 5 mM EDTA, 5 mM EGTA, 15 mM $MgCl_2$, 60 mM β-glycerophosphate, 0.1 mM sodium orthovanadate, 0.1 mM NaF, 0.1 mM benzamide, 10 μg/ml aprotinin, 10 μg/ml leupeptin, and 1 mM PMSF). Detergent-insoluble materials were removed by centrifugation at 12,000*g* for 10 min at 4°C. Protein concentrations were determined by the Lowry assay, 500 μg of total cell lysates were incubated with primary antibody at 4°C for 2 h. Pre-equilibrated proteinA/G-agarose beads (Santa Cruz) were then added and incubated overnight. They were collected by centrifugation at 12,000*g* and gently washed three times with the lysis buffer. The bound proteins were eluted by boiling in 2 × SDS sample buffer, and then performed Western blotting analysis according to the standard protocols.

For tyrosine phosphorylation level of β-catenin analysis, cells were cultured for 24 h in a DMEM medium containing 1% fetal calf serum. After 50 ng/ml EGF (Promega) was added for the indicated times, cells were collected and β-catenin was separated by immunoprecipitation with an antibody against β-catenin (Santa Cruz). Tyrosine phosphorylation level of β-catenin was analyzed by Western blotting using an anti-phosphotyrosine antibody, PY20 (Santa Cruz). The PVDF membrane was re-probed with the antibody against β-catenin to verify that equal amount of precipitated protein was obtained.

## RESULTS

### All Four Potential *N*-Glycosylation Sites of E-Cadherin Are *N*-Glycosylated

The ectodomain of human E-cadherin contains four potential *N*-glycosylation sites at Asn

residues 554, 566, 618, and 633 on the basis of amino acid sequence analysis (GenBank Accession L08599) [Rimm and Morpanels, 1994]. To date, little has been known about the role of *N*-glycosylation in E-cadherin-mediated cell–cell adhesion. Here we obliterated each consensus sequence by substituting Gln for Asn, either individually or in combination (Fig. 1A). This method is generally considered to lead to the least perturbation of protein function. The E-cadherin mutants with one individual *N*-glycosylation site abrogated (M1-Ecad, N554Q; M2-Ecad, N566Q; M3-Ecad, N618Q; M4-Ecad, N633Q) and several *N*-glycosylation sites abrogated in combination (M123-Ecad, N554QN566QN618Q; M1234-Ecad, N554QN566QN618QN633Q) were stably expressed in human breast carcinoma MDA-MB-435 cells, which lack E-cadherin expression at both the mRNA and protein levels (Fig. 1B) [Liu et al., 1997].

We first investigated whether all four potential *N*-glycosylation sites of E-cadherin were occupied in MDA-MB-435 cells. As shown in Figure 1C, all E-cadherin mutants with a single *N*-glycosylation site abrogated (except M4-Ecad mutant) demonstrated increased mobility on Western blotting compared with wild-type E-cadherin, which indicated that potential *N*-glycosylation sites at Asn-554, Asn-566, and Asn-618 of human E-cadherin were *N*-glycosylated in MDA-MB-435 cells. Moreover, the most pronounced mobility changes were observed for M1-Ecad mutant followed by M2-Ecad and M3-Ecad mutants, which suggested that *N*-glycan at Asn-554 of E-cadherin was most substantial in size.

However, it was difficult to observe the mobility changes of M4-Ecad mutant for its undetectable protein band (Fig. 1C). Thus, MALDI-TOF MS was performed to determine the occupation of *N*-glycosylation site at Asn-633 of E-cadherin. E-cadherin mutant lacking *N*-glycans at Asn-554, Asn-566, and Asn-618 (M123-Ecad mutant) was purified and digested with *N*-glycosidase F (PNGaseF) to release the glycan portion, thus allowing analysis of the deglycosylated peptides by MALDI-TOF MS. As shown in Figure 1D, the spectrum revealed four complex patterns of signals and the assignment of the monosaccharide compositions in these peaks. The signals at *m/z* 1663.38, *m/z* 1843.85, *m/z* 2005.17, and *m/z* 2344.0 were in agreement with oligosaccharide structures $HexNAc_3Man_3GlcNAc_2$, $HexNAc_4Man_3GlcNAc_2$, $Hex_1HexNAc_4Man_3GlcNAc_2$, and $Hex_2HexNAc_2NeuAC_2Man_3GlcNAc_2$, respectively. Part of putative *N*-glycans structures was also presented in Figure 1D. These data confirmed that the potential *N*-glycosylation site at Asn-633 of E-cadherin was occupied by complex *N*-glycan in MDA-MB-435 cells.

As illustrated in Figure 1C, E-cadherin protein bands in M4-Ecad-435 and M1234-Ecad-435 cells were very faint or even undetectable, whereas the mRNA levels of E-cadherin in these two transfectants were similar to that in wtEcad-435 cells. This discrepancy of E-cadherin protein and mRNA levels could be repeated in many other transfectants of these two cell lines (data not shown). On the other hand, M123-Ecad mutant with the presence of single *N*-glycan at Asn-633 could be expressed at both the mRNA and protein levels. These findings implied that Asn-633-linked *N*-glycan seems to be required for E-cadherin stability. To detect the effect of the other three *N*-glycans on the stability of E-cadherin, we analyzed the stability of M123-Ecad mutant by cycloheximide (CHX) treatment. CHX (50 μg/ml) was added to wtEcad-435 and M123-Ecad-435 cells for 12 h to inhibit new protein synthesis. The total protein lysates were then collected at the indicated time (0, 2, 4, 6, and 8 h) and subjected to Western blotting analysis. As shown in Figure 1E,F, the half-life of M123-Ecad mutant was similar to that of wild-type E-cadherin. These results demonstrated *N*-glycans at Asn-554, Asn-566, and Asn-618 contribute slightly to E-cadherin stability.

### *N*-Glycosylation Affects the Adhesive Function of E-Cadherin

We next examined the role of *N*-glycosylation in the adhesive function of E-cadherin using cell aggregation assay. The rate of calcium-dependent cell–cell adhesion was measured by AI as mentioned above. As shown in Figure 2A,B, calcium-dependent cell–cell adhesion of M1-Ecad-435, M2-Ecad-435 and M123-Ecad-435 cells was significantly lower than that of wtEcad-435 cells. Moreover, calcium-dependent cell–cell adhesion of M1-Ecad-435 cells was especially lower than that of M2-Ecad-435 cells. Previous studies demonstrated that E-cadherin-mediated cell–cell adhesion prevents migration and invasion of human carcinoma cells [Christofori and Semb, 1999]. Here we found M1-Ecad-435 and

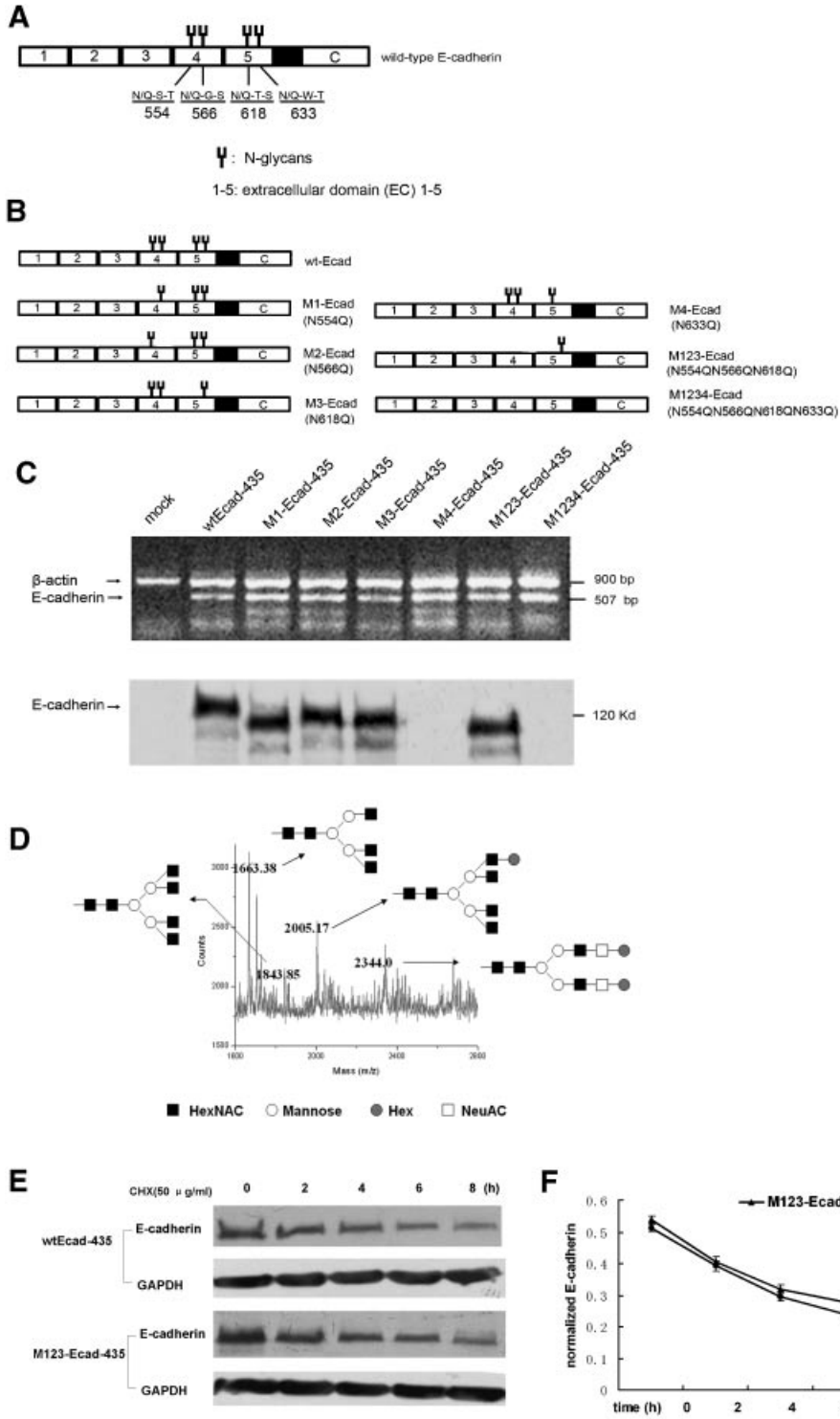


**Fig. 1.** The four potential *N*-glycosylation sites at Asn residues 554, 566, 618, and 633 of human E-cadherin were *N*-glycosylated in MDA-MB-435 cells. **A**,**B**: Schematic representation of site-directed mutagenesis (A) and *N*-glycosylation-deficient mutants of E-cadherin (B). **C**: The mRNA levels of E-cadherin in *N*-glycosylation-deficient mutants of E-cadherin were detected by RT-PCR (the **upper panels**). The protein levels of E-cadherin in *N*-glycosylation-deficient mutants of E-cadherin were detected by Western blotting (the **lower panels**). **D**: The occupation of *N*-glycosylation site at Asn-633 of E-cadherin were investigated by MALDI-TOF MS. Due to *N*-glycans were labeled with 2-anthrailic acid (2-AA, FW = 137.14) before analysis on MALDI-TOF MS, the mass of annotated structure was off about 137.14 from the *m*/*z* of each peak. **E**,**F**: Analysis of protein stability of wild-type E-cadherin and M123-Ecad mutant. wtEcad-435 and M123-Ecad-435 cells were treated with 50 μg/ml CHX for 12 h, and total cell lysates were collected at the indicated time points and subjected to Western blotting. A typical blot (E) and densitometric scans of triplicate blots (F) are shown. Data are presented as mean ± SD.

M2-Ecad-435 cells exhibited increased cell migration capacity along with disruption of cell–cell adhesion (Fig. 2C,D). Nevertheless, no difference was observed in the rates of cell–cell adhesion and cell migration between wtEcad-435 and M123-Ecad-435 cells (Fig. 2A–D). Overall, these findings suggested that *N*-glycans at Asn-554 and Asn-566, but not Asn-618, significantly affect the adhesive function of E-cadherin.

Previous reports showed that MDA-MB-435 cells express a moderate level of N-cadherin instead of E-cadherin [Fedor-Chaiken et al., 2003]. In some studies, the re-expression of E-cadherin in E-cadherin-negative tumor cells was shown to downregulate the endogenous N-cadherin expression [Kuphal and Bosserhoff, 2006]. Here the expression of N-cadherin in mock, wtEcad-435 and M123-Ecad-435 cells was detected using Western blotting analysis. These data showed that the above cell lines expressed N-cadherin at the similar level (Fig. 3A), which suggested that the re-expression of wild-type E-cadherin or M123-Ecad mutant did not affect the expression of endogenous N-cadherin in MDA-MB-435 cells.

To further exclude the possible involvement of integrin and N-cadherin in reduced calcium-dependent cell–cell adhesion of M123-Ecad-435 cells, we used function-blocking antibodies in

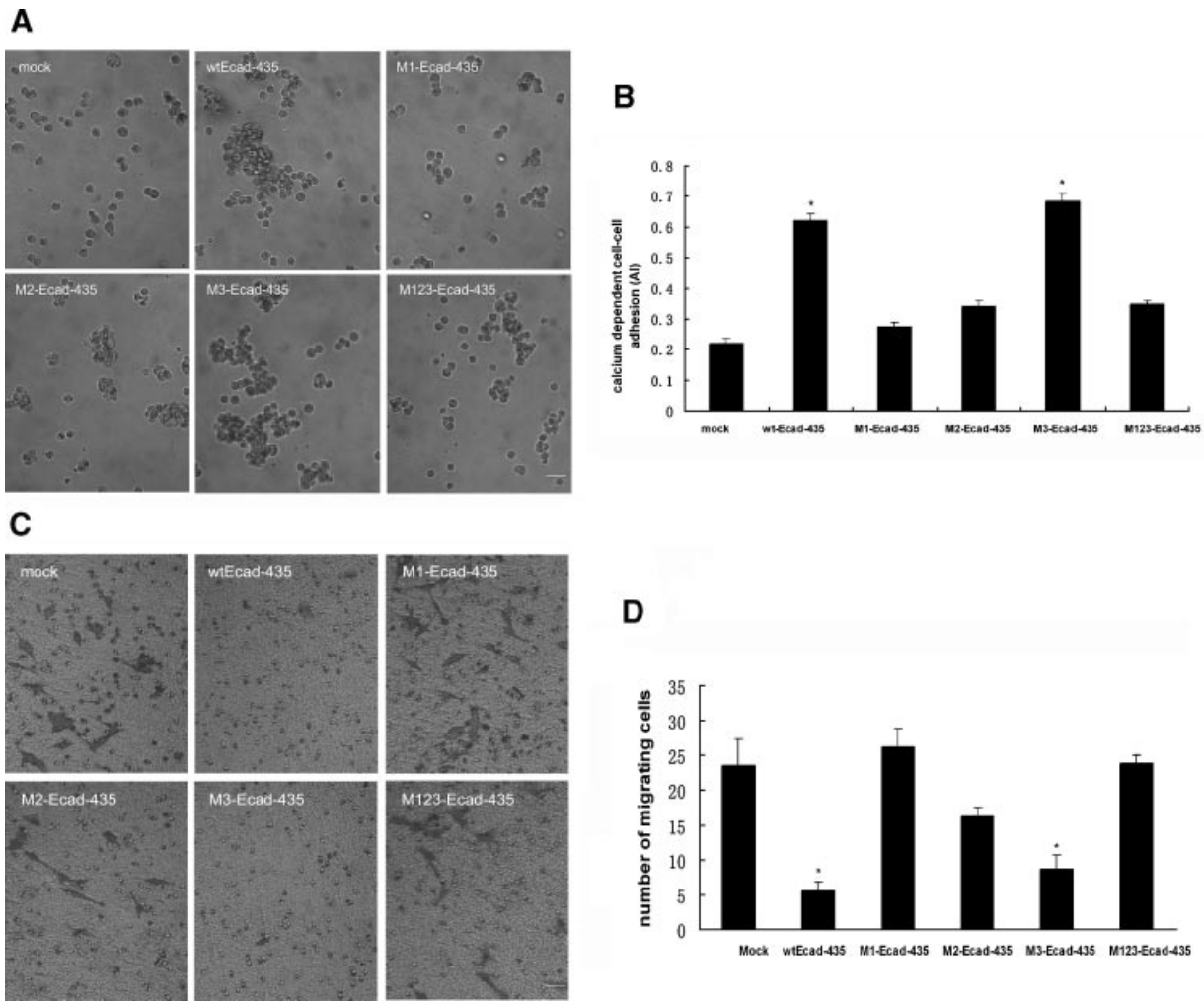


**Fig. 2.** *N*-glycans at Asn-554 and Asn-566 affected the adhesive function of E-cadherin. **A**: Calcium-dependent cell–cell adhesion of mock, wtEcad-435, M1-Ecad-435, M2-Ecad-435, M3-Ecad-435, and M123-Ecad-435 cells was analyzed by cell aggregation assay. Scale bar = 20 μm. **B**: Quantitative representation of cell aggregation assay (A). Data represent mean ± SD of three independent experiments. $^*P < 0.05$, compared with mock cells. **C**: Cell migration of the above six cell lines was investigated using cell migration assay. Scale bar = 20 μm. **D**: Quantitative representation of cell migration assay (C). Data are also presented as mean ± SD from three independent experiments. $^*P < 0.05$, compared with mock cells.

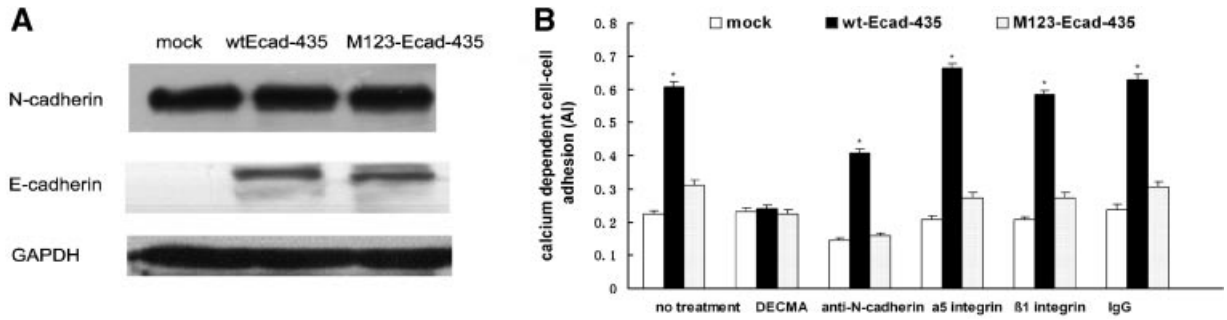


**Fig. 3.** Reduced cell–cell adhesion in M123-Ecad-435 cells was due to the changes of *N*-glycan moiety of E-cadherin, not to N-cadherin or integrin. **A**: The N-cadherin expression in mock, wtEcad-435 and M123-Ecad-435 cells was detected by Western blotting. The GAPDH was used as a loading control. **B**: Effects of potential inhibitors on calcium-dependent cell–cell adhesion of the above cells. Protein inhibitors used here are function-blocking antibodies against N-cadherin, E-cadherin (DECMA), α5 integrin, β1 integrin, and nonimmune IgG was used as a control. These antibodies were added into the cell suspension respectively and cells were allowed to aggregate for 30 min at 37°C with 80 rpm agitation. The results (mean ± SD) of three independent experiments are shown. $*P < 0.05$, compared with mock cells.

cell aggregation assay. As shown in Figure 3B, calcium-dependent cell–cell adhesion of mock, wtEcad-435 and M123-Ecad-435 cells was unaffected by antibodies against α5 integrin and β1 integrin. Meanwhile, although function-blocking antibody of N-cadherin was shown to inhibit calcium-dependent cell–cell adhesion of these cell lines, it could not eliminate the difference in calcium-dependent cell–cell adhesion between wtEcad-435 and M123-Ecad-435 cells. In contrast, function-blocking antibody against E-cadherin (DECMA) significantly inhibited calcium-dependent cell–cell adhesion of wtEcad-435 and M123-Ecad-435 cells and eliminated the difference in calcium-dependent cell–cell adhesion between the two cell lines. Together, these findings suggested that lower capacity of cell–cell adhesion of M123-Ecad-435 cells was mainly due to the changes of *N*-glycan moiety of E-cadherin, not to integrin or N-cadherin.

### E-Cadherin *N*-Glycosylation Affects Tyrosine Phosphorylation of β-Catenin

Next, we investigated the mechanisms by which E-cadherin *N*-glycosylation affected calcium-dependent cell–cell adhesion. E-cadherin is not always at AJs, and it spends variable amounts of time in vesicles trafficking to and from the cell surface. E-cadherin on the cell surface, instead of those in intracellular vesicles and compartments, plays a crucial role in mediating cell–cell adhesion [Bryant and Stow, 2004]. Consequently, we wanted to know whether *N*-glycans at Asn-554, Asn-566, and Asn-618 affected the correct localization of E-cadherin to the cell surface, and ultimately led to disruption of cell–cell adhesion. To this end, immunofluorescence analysis was performed and these data suggested that *N*-glycans at Asn-554, Asn-566, and Asn-618 do not affect the localization of E-cadherin to the cell surface (data not shown).

The highly conserved cytoplasmic region of E-cadherin interacts with β-, α-, and γ-catenins, which mediate connections between E-cadherin and the actin cytoskeleton and ultimately form cell–cell adhesion [Provost and Rimm, 1999; Nagafuchi, 2001]. Cell–cell adhesion is a rather dynamic process for which interactions between cell adhesion molecules and the actin cytoskeleton must be continually modified. E-cadherin and especially β-catenin are major target sites for phosphorylation and dephosphorylation modifications [Gumbiner, 2000; Lilien and Balsamo, 2005].

In our study, tyrosine phosphorylation levels of β-catenin in 435, mock, wtEcad-435 and M123-Ecad-435 cells were then investigated with epidermal growth factor (EGF) as a stimulus. Previous studies reported that EGF can induce a rapid tyrosine phosphorylation of β-catenin [Hazan and Norton, 1998]. When treated with EGF (50 ng/ml), wtEcad-435 and M123-Ecad-435 cells showed no difference in total protein levels of β-catenin (data not shown). However, a marked difference in tyrosine phosphorylation of β-catenin was observed between two cell lines. The tyrosine phosphorylation level of β-catenin in wtEcad-435 cells was very low and increased slightly after EGF stimulation. In case of M123-Ecad-435

cells, the basal level of tyrosine phosphorylation of β-catenin before EGF treatment was somewhat higher than that in wtEcad-435 cells, and it increased dramatically after EGF stimulation and persisted for at least 60 min (Fig. 4A,B).

In order to further elucidate the extent of involvement of E-cadherin *N*-glycosylation in tyrosine phosphorylation of β-catenin, we treated wtEcad-435 and M123-Ecad-435 cells with tunicamycin (TM) before the addition of EGF. Tunicamycin (TM) used here could produce the similar *N*-glycans structures of E-cadherin in wtEcad-435 and M123-Ecad-435 cells by blocking the first step in biosynthesis of the lipid-linked oligosaccharide precursor. And we found that the patterns of tyrosine phosphorylation of β-catenin in wtEcad-435 and M123-Ecad-435 cells seemed to be almost identical after TM treatment (Fig. 4C,D), which indicated that the difference in tyrosine phosphorylation of β-catenin between two cell lines was mainly attributed to the presence of differential *N*-glycans on E-cadherin. Together, these results suggested a direct involvement of E-cadherin *N*-glycosylation in tyrosine phosphorylation of β-catenin.

### E-Cadherin *N*-Glycosylation Affects the Composition of AJs

The above data provided evidence that removal of *N*-glycans on E-cadherin resulted in elevated tyrosine phosphorylation of β-catenin. Considering that enhanced tyrosine phosphorylation level of β-catenin was usually viewed as a concomitant with the disassociation of cadherin–catenin complex [Matsuyoshi

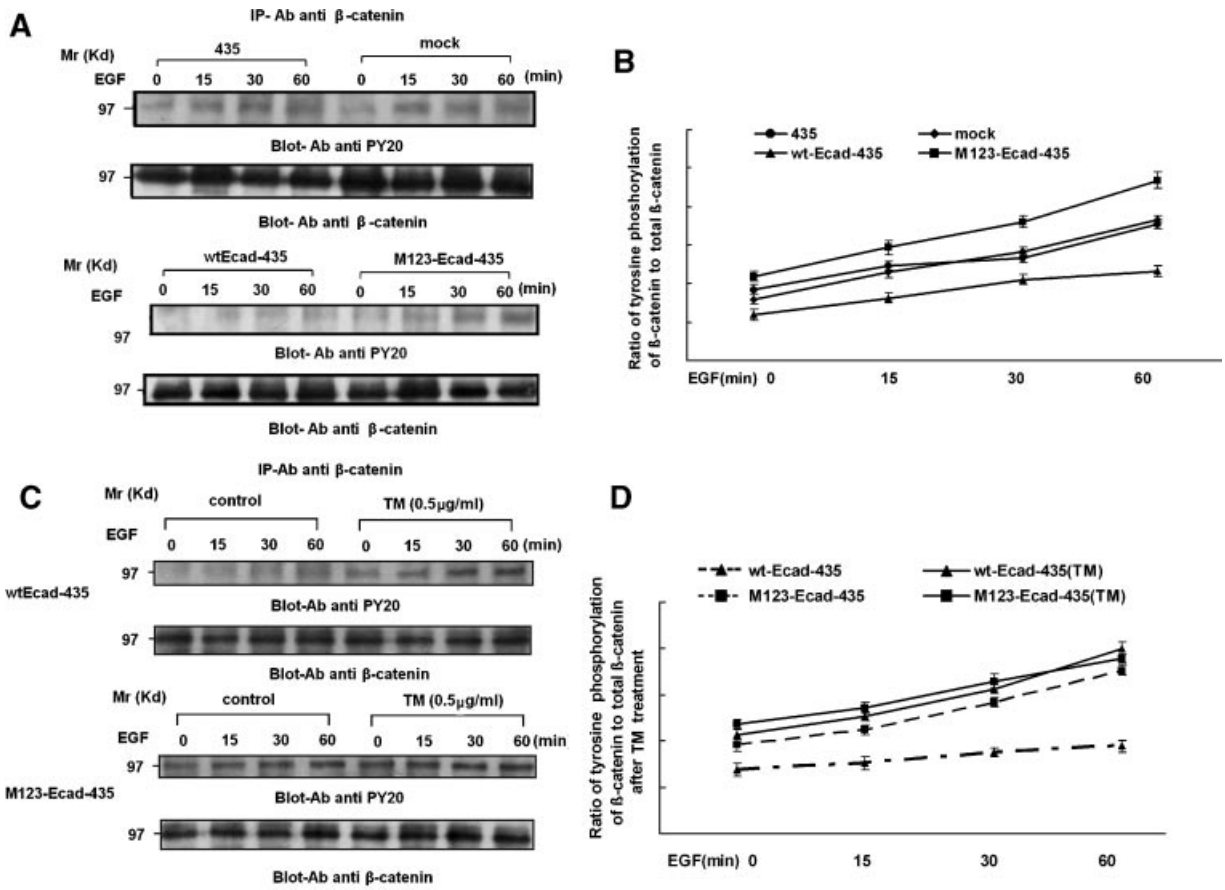


**Fig. 4.** Removal of *N*-glycosylation on E-cadherin resulted in elevated tyrosine phosphorylation level of β-catenin. **A**,**B**: Tyrosine phosphorylation levels of β-catenin in 435, mock, wtEcad-435, and M123-Ecad-435 cells were investigated by immunoprecipitation. A typical blot (A) and densitometric scans of triplicate blots (B) are shown. Data are presented as mean ± SD. **C**,**D**: Tyrosine phosphorylation levels of β-catenin in the above cell lines after TM treatment were detected by immunoprecipitation. Cells were treated with tunicamycin (TM, 0.5 mg/ml) for 24 h, then stimulated with EGF (50 ng/ml) for the indicated times. A typical blot (C) and densitometric scans of triplicate blots (D) are shown. Data are also presented as mean ± SD.

et al., 1992; Behrens et al., 1993; Hoschuetzky et al., 1994; Ozawa and Kemler, 1998], we hypothesized that removal of *N*-glycans of E-cadherin would lead to an increase in tyrosine phosphorylation of β-catenin, which maybe, in turn, affected the composition of AJs. To confirm this hypothesis, we first investigated whether *N*-glycans at Asn-554, Asn-566, and Asn-618 of E-cadherin affected the formation of E-cadherin/β-catenin complex using immunoprecipitation assay. As shown in Figure 5A, M123-Ecad mutant could bind to β-catenin as wild-type E-cadherin.

Further, we compared the composition of AJs formed by wild-type E-cadherin with that formed by M123-Ecad mutant. Since E-cadherin in the Triton X-100-insoluble cytoskeletal fractions has been shown previously to reach AJs and anchor to the actin cytoskeleton [McNefll et al., 1993; Hinck et al., 1994; Bryant and Stow, 2004], 1% Triton X-100 was used to extract E-cadherin-based AJs fractions. In view that cell confluence influenced recruitment of E-cadherin to the cell surface [Le et al., 1999], Triton X-100-insoluble cytoskeletal fractions derived from wtEcad-435 and M123-Ecad-435 cells which were grown and maintained under different conditions (dense conditions: cells were grown to >90% confluence; sparse conditions: cells were grown to <30% confluence) were prepared respectively. As shown in Figure 5B, despite E-cadherin at AJs was substantially increased in both wtEcad-435 and M123-Ecad-435 cells cultured under dense conditions compared with those under sparse conditions, the levels of β- and α-catenins at AJs in M123-Ecad-435 cells (Fig. 5B), as well as the ratio of β- and α-catenins to E-cadherin (Fig. 5C,D), were significantly lower than those in wtE-cad-435 cells under the same conditions. As mentioned before, β-catenin links E-cadherin to the actin cytoskeleton, which forms calcium-dependent cell–cell adhesion. Therefore, we hypothesized that removal of *N*-glycans of E-cadherin may modify the composition of β- and α-catenin at AJs, which further resulted in reduced calcium-dependent cell–cell adhesion.

## DISCUSSION

E-cadherin, an important member of the cadherin family, provides calcium-dependent cell–cell adhesion between adjacent epithelial cells [Provost and Rimm, 1999; Nagafuchi, 2001]. The ectodomain of human E-cadherin contains four potential *N*-glycosylation sites at Asn residues 554, 566, 618, and 633. Herein *N*-glycosylation-deficient mutants of E-cadherin were generated by substituting Asn by Gln in the consensus sequence NXS/T and then the role of E-cadherin *N*-glycosylation in its adhesive function and the molecular mechanisms were investigated in detail.

In this study, we found that *N*-glycans at Asn-554 and Asn-566 affect the adhesive function of E-cadherin in MDA-MB-435 cells. To explore the mechanisms underlying this phenomenon, we examined the effect of *N*-glycosylation on the intracellular localization of E-cadherin. Protein *N*-glycosylation has long been known to ensure proper protein folding and intracellular localization for influenza hemagglutinin [Roberts et al., 1993], CD39 and glycine transporter (GLYT2) [Zhong et al., 2001; Martinez-Maza et al., 2001]. However, such a function of *N*-glycosylation was not found for type VI adenylyl cyclase (ACVI) and the Lassa virus glycoprotein GP-C [Wu et al., 2001; Eichler et al., 2006]. Using immunofluorescence analysis, we found that *N*-glycans at Asn-554, Asn-566, and Asn-618 do not affect the correct localization of E-cadherin to the cell surface.

β-catenin, as a key mediator of the Wnt signaling pathway, has been shown to play a dual role in E-cadherin-mediated cell–cell adhesion [Miller et al., 1999; Zhurinsky et al., 2000; Gottardi and Gumbiner, 2004; Harris and Peifer, 2005]. It binds tightly to the cytoplasmic domain of E-cadherin and then to α-catenin and vinculin, through which adherens complex is linked to the actin cytoskeleton [Provost and Rimm, 1999; Nagafuchi, 2001; Gottardi and Gumbiner, 2004; Harris and Peifer, 2005]. E-cadherin/β-catenin complex forms immediately after the synthesis of E-cadherin and α-catenin associates with E-cadherin/β-catenin complex later in the secretory pathway [McCrea et al., 1991; Ozawa and Kemler, 1992]. E-cadherin-mediated cell–cell adhesion is a rather dynamic process that is regulated by diverse factors. E-cadherin and especially β-catenin are major target sites for modifications of cell–cell adhesion, including primarily phosphorylation and dephosphorylation events [Lilien and Balsamo, 2005; Gumbiner, 2000]. Elevated serine/threonine phosphorylation

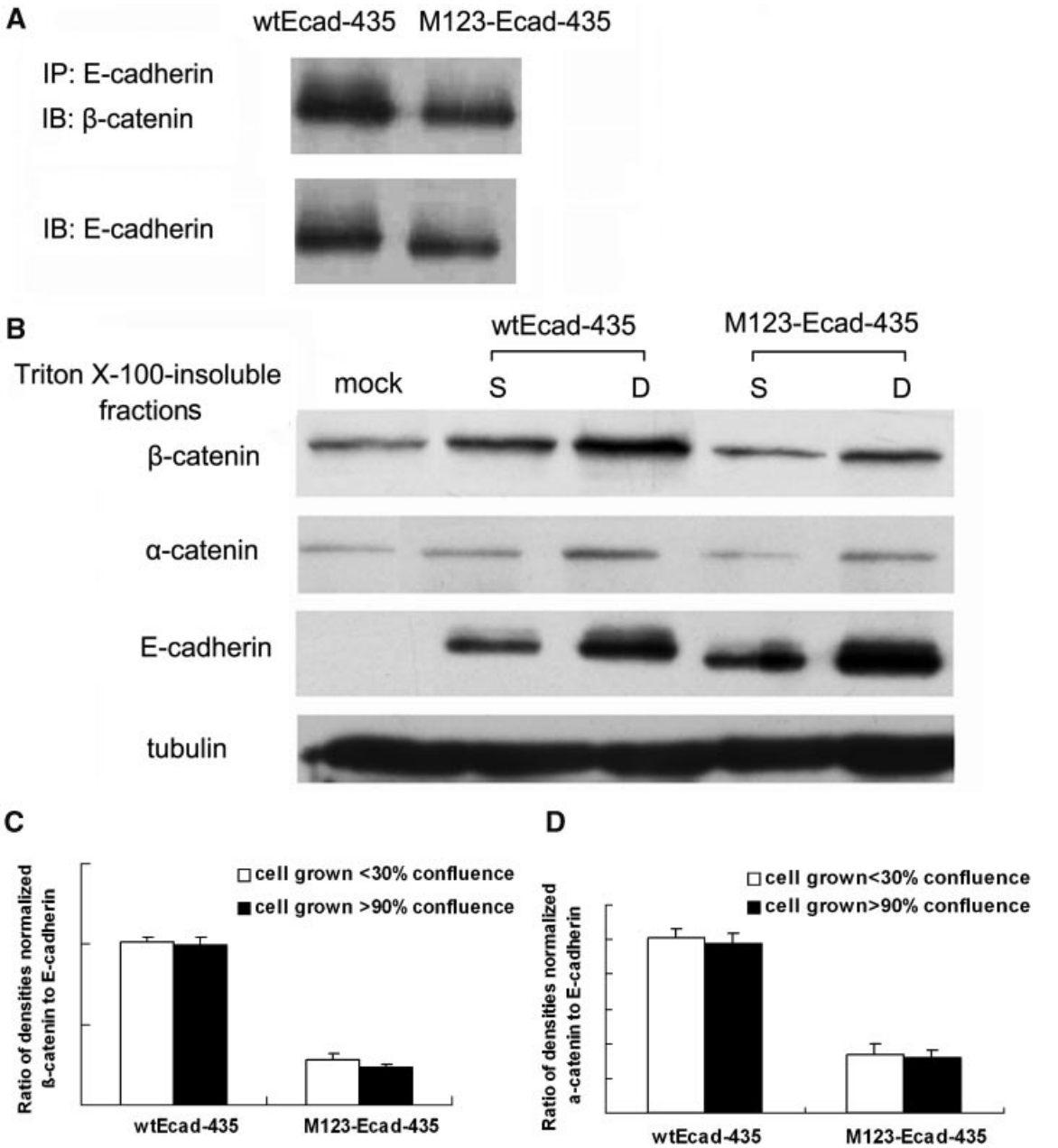


**Fig. 5.** Removal of *N*-glycosylation on E-cadherin resulted in reduced β- and α-catenins at AJs. **A**: The binding of M123-Ecad mutant to β-catenin was determined by immunoprecipitation. Cell lysates from wtEcad-435 and M123-Ecad-435 cells were immunoprecipitated with anti-E-cadherin antibody, and followed by Western blotting with the antibody against E-cadherin and β-catenin. Representative results from one of two experiments are shown. **B**: The composition of AJs formed by wild-type E-cadherin and that formed by M123-Ecad mutant. Mock, wtEcad-435 and M123-Ecad-435 cells were grown and maintained at different densities. S, sparse conditions; D, dense conditions. Triton X-100-insoluble cytoskeletal fractions from the above cell lines were prepared and underwent Western blotting analysis. The primary antibodies used here was indicated left. The tubulin was regarded as a loading control. **C**,**D**: Quantitative analyses of the ratio of β-catenin to E-cadherin (C) and the ratio of α-catenin to E-cadherin (D) at AJs in wtEcad-435 and M123-Ecad-435 cells. Data represent mean ± SD of three independent experiments.

levels of E-cadherin result in increased stabilization of E-cadherin/β-catenin complex and increased E-cadherin-mediated cell–cell adhesion [Lickert et al., 2000; Serres et al., 2000; Bek and Kemler, 2002]. When E-cadherin was phosphorylated by casein kinase II (CKII) or glycogen synthase kinase-3b (GSK-3b), the interaction between E-cadherin and β-catenin

was enhanced and cell–cell adhesion was strengthened [Lickert et al., 2000]. In our study removal of *N*-glycans of E-cadherin did not influence serine/threonine phosphorylation levels of E-cadherin (data not shown), but it caused an increase in tyrosine phosphorylation levels of β-catenin.

Consistent with our findings, previous studies showed that modifications of E-cadherin *N*-glycosylation by GnT III resulted in decreased tyrosine phosphorylation of β-catenin [Kitada et al., 2001]. Then, how *N*-glycosylation of E-cadherin affects tyrosine phosphorylation levels of β-catenin? One possible mechanism is that *N*-glycosylation directly affects the spatial conformation of E-cadherin/β-catenin adhesion complex. In addition, previous studies demonstrated that there was bi-directional regulation between receptor tyrosine kinases (RTKs) and E-cadherin [Qian et al., 2004; Andl and Rustgi, 2005]. The ectodomain of E-cadherin seems to be crucial for the inhibition of E-cadherin to RTKs. Truncation mutations of the ectodomain of E-cadherin potentially caused upregulation of RTKs activity in infiltrative lobular breast carcinomas [Berx et al., 1995]. Thus, *N*-glycosylation of E-cadherin may affect the inhibitory effect of E-cadherin on RTKs by modifying spatial conformation of the ectodomain of E-cadherin.

It is widely accepted that elevated tyrosine phosphorylation levels of β-catenin induce disassociation of E-cadherin/β-catenin complex. Data from different groups have confirmed a strong correlation between elevated tyrosine phosphorylation levels of β-catenin and disruption of cell–cell adhesion [Matsuyoshi et al., 1992; Behrens et al., 1993; Hoschuetzky et al., 1994; Ozawa and Kemler, 1998]. Along with the decreased β- and α-catenins at AJs (Fig. 5B,C), we hypothesize that E-cadherin *N*-glycosylation may influence the composition of AJs through modifying tyrosine phosphorylation levels of β-catenin, and ultimately affect E-cadherin-mediated cell–cell adhesion.

Actually, Liwosz et al. [2006] had different observations in another similar study and they found that E-cadherin *N*-glycosylation destabilized AJs in Chinese Hamster Ovary (CHO) and Madin–Darby canine kidney (MDCK) cell lines. Notably, both CHO and MDCK cell lines are glycosylation-defective mammalian cell lines. For instance, CHO cell line is defective in Golgi *N*-acetylglucosaminyltransferase III (GnT III) and α 1,3-fucosyltransferase activity. Accordingly, glycoproteins processed in CHO cell lines are defective in bisecting glycans and peripheral fucose residues. On the other hand, *N*-glycosylation is often altered in all types of human cancers. For this reason, *N*-glycans structures of E-cadherin expressed in human breast carcinoma MDA-MB-435 cells are obvious distinct from that expressed in CHO and MDCK cells. Therefore, it is understandable that *N*-glycosylation of E-cadherin in different cells presumably has distinct influences on its adhesive function. In other words, the role of *N*-glycosylation of E-cadherin in regulation of E-cadherin-associated cell–cell adhesion depends on specific *N*-glycans structures of E-cadherin which could be differential in different types of cells.

In addition, vinculin may be involved in regulation of E-cadherin *N*-glycosylation to cell–cell adhesion [Liwosz et al., 2006]. It is a membrane-cytoskeletal protein which assembles in the adhesion complex by direct binding to β-catenin and competing with α-catenin for the same binding site on β-catenin and mediates the linkage of β-catenin to the actin cytoskeleton [Hazan et al., 1997]. Since no evidence supports that vinculin is able to bind to E-cadherin directly, it seems that *N*-glycosylation of E-cadherin modulates the recruitment of vinculin at AJs in an indirect manner.

## ACKNOWLEDGMENTS

The authors thank Dr. Cara J. Gottardi for his gifts of Human E-cadherin cDNA plasmid as well as Dr. Tongzhong Ju and Dr. Baoyun Xia for their kindly assistance with MALDI-TOF MS analysis.

## REFERENCES

Andl CD, Rustgi AK. 2005. No one-way street: Cross-talk between E-cadherin and receptor tyrosine kinase (RTK) signaling: A mechanism to regulate RTK activity. Cancer Biol Ther 4:28–31.

Behrens J, Vakaet L, Friis R, Winterhager E, Vanroy F, Mareel MM, Birchmeier W. 1993. Loss of epithelial differentiation and gain of invasiveness correlates with tyrosine phosphorylation of the E-cadherin/beta-catenin complex in cells transformed with a temperature-sensitive v-SRC gene. J Cell Biol 120:757–766.

Bek S, Kemler R. 2002. Protein kinase CKII regulates the interaction of β-catenin with α-catenin and its protein stability. J Cell Sci 115:4743–4753.

Berx G, Cleton-Jansen AM, Nollet F, de Leeuw WJF, van de Vijver MJ, Cornelisse C, van Roy F. 1995. E-cadherin is a tumor/invasion suppressor gene mutated in human lobular breast cancers. EMBO J 14:6107–6115.

Bourguignon LY, Zhu H, Shao L, Chen YW. 2000. CD44 interaction with tiam1 promotes Rac1 signaling and hyaluronic acid-mediated breast tumor cell migration. J Biol Chem 275:1829–1838.

Bryant DM, Stow JL. 2004. The ins and outs of E-cadherin trafficking. Trends Cell Biol 14:427–434.

Christofori G, Semb H. 1999. The role of the cell adhesion molecule E-cadherin as a tumor suppressor gene. Trends Biochem Sci 24:73–76.

Eichler R, Lenz O, Garten W, Strecker T. 2006. The role of single N-glycans in proteolytic processing and cell surface transport of the Lassa virus glycoprotein GP-C. Virol J 3:41.

Fedor-Chaiken M, Meigs TE, Kaplan DD, Brackenbury R. 2003. Two regions of cadherin cytoplasmic domains are involved in suppressing motility of a mammary carcinoma cell line. J Biol Chem 278:52371–52378.

Gottardi CJ, Gumbiner BM. 2004. Distinct molecular forms of beta-catenin are targeted to adhesive or transcriptional complexes. J Cell Biol 167:339–349.

Gottardi CJ, Wong E, Gumbiner BM. 2001. E-cadherin suppresses cellular transformation by inhibiting beta-catenin signaling in an adhesion-independent manner. J Cell Biol 153:1049–1060.

Gumbiner BM. 2000. Regulation of cadherin adhesive activity. J Cell Biol 148:399–403.

Gumbiner BM. 2005. Regulation of cadherin-mediated adhesion in morphogenesis. Nat Rev Mol Cell Biol 6: 622–633.

Guo HB, Lee I, Kamar M, Pierce M. 2003. N-acetylglucosaminyltransferase V expression levels regulate cadherin-associated homotypic cell-cell adhesion and intracellular signaling pathways. J Biol Chem 78: 52412–52424.

Harris TJ, Peifer M. 2005. Decisions, decisions: Beta-catenin chooses between adhesion and transcription. Trends Cell Biol 15:234–237.

Hazan RB, Norton L. 1998. The epidermal growth factor receptor modulates the interaction of E-cadherin with the actin cytoskeleton. J Biol Chem 273:9078–9084.

Hazan RB, Kang L, Roe S, Borgen PI, Rimm DL. 1997. Vinculin is associated with the E-cadherin adhesion complex. J Biol Chem 272:32448–32453.

Helenius A, Aebi M. 2004. Roles of N-linked glycans in the endoplasmic reticulum. Annu Rev Biochem 73:1019–1049.

Hinck L, Nathke IS, Papkoff J, Nelson WJ. 1994. Dynamics of cadherin/catenin complex formation: Novel protein interactions and pathways of complex assembly. J Cell Biol 125:1327–1340.

Hoschuetzky H, Aberle H, Kemler R. 1994. Beta-catenin mediates the interaction of the cadherin-catenin complex with epidermal growth factor receptor. J Cell Biol 127: 1375–1380.

Kim DY, Ingano LA, Kovacs DM. 2002. Nectin-1 alpha, an immunoglobulin-like receptor involved in the formation of synapses, is a substrate for presenilin/gammasecretase-like cleavage. J Biol Chem 277:49976–49981.

Kitada T, Miyoshi E, Noda K, Higashiyama S, Ihara H, Matsuura N, Hayashi N, Kawata S, Matsuzawz Y, Taniguchi N. 2001. The addition of bisecting N-acetylglucosamine residues to E-cadherin down-regulates the tyrosine phosphorylation of β-catenin. J Biol Chem 276: 475–480.

Kuphal S, Bosserhoff AK. 2006. Influence of the cytoplasmic domain of E-cadherin on endogenous N-cadherin expression in malignant melanoma. Oncogene 25:248–259.

Le TL, Yap AS, Stow JL. 1999. Recycling of E-cadherin: A potential mechanism for regulating cadherin dynamics. J Cell Biol 146:219–232.

Liang YL, Fu Y, Chen SG, Cai XM, Su JM, Jin JW, Ma DZ, Li ZX, Zhang W, Zha XL. 2004. Integrin β1 subunit overexpressed in the SMMC-7721 cells regulates the promoter activity of p21CIP1 and enhances its transcription. FEBS Lett 558:107–113.

Lickert H, Bauer A, Kemler R, Stappert J. 2000. Casein kinase II phosphorylation of E-cadherin increases E-cadherin/β-catenin interaction and strengthens cell-cell adhesion. J Biol Chem 275:5090–5095.

Lilien J, Balsamo J. 2005. The regulation of cadherin-mediated adhesion by tyrosine phosphorylation/dephosphorylation of beta-catenin. Curr Opin Cell Biol 17:459–465.

Liu Z, Brattain MG, Appert H. 1997. Differential display of reticulocalbin in the highly invasive cell line, MDA-MB-435, versus the poorly invasive cell line, MCF-7. Biochem Biophys Res Commun 231:283–289.

Liwosz A, Lei T, Kukuruzinska MA. 2006. N-glycosylation affects the molecular organization and stability of E-cadherin junctions. J Biol Chem 281:23138–23149.

Makagiansar IT, Nguyen PD, Ikesue A, Kuczera K, Dentler W, Urbauer JL, Galeva N, Alterman M, Siahaan TJ. 2002. Disulfide bond formation promotes the cis- and trans-dimerization of the E-cadherin-derived first repeat. J Biol Chem 277:16002–16610.

Martinez-Maza R, Poyatos I, López-Corcuera B, Núñez E, Giménez C, Zafra F, Aragón C. 2001. The role of N-glycosylation in transport to the plasma membrane and sorting of the neuronal glycine transporter GL YT2. J Biol Chem 276:2168–2173.

Matsuyoshi N, Hamaguchi M, Taniguchi S, Nagafuchi A, Tsukita S, Takeichi M. 1992. Cadherin-mediated cell-cell adhesion is perturbed by v-src tyrosine phosphorylation in metastatic fibroblasts. J Cell Biol 118:703–714.

McCrea PD, Turck CW, Gumbiner B. 1991. A homolog of the armadillo protein in Drosophila (plakoglobin) associated with E-cadherin. Science 254:1359–1361.

McNefll H, Ryan TA, Smith SJ, Nelson WJ. 1993. Spatial and temporal dissection of immediate and early events following cadherin-mediated epithelial cell adhesion. J Cell Biol 120:1217–1226.

Miller JR, Hocking AM, Bpanelsn JD, Moon RT. 1999. Mechanism and function of signal transduction by the Wnt/beta-catenin and Wnt/Ca2+ pathways. Oncogene 18:7860–7872.

Nagafuchi A. 2001. Molecular architecture of adherens junctions. Curr Opin Cell Biol 13:600–603.

Nose A, Tsuji K, Takeichi M. 1990. Localization of specificity determining sites in cadherin cell adhesion molecules. Cell 61:147–155.

Ozawa M, Kemler R. 1992. Molecular organization of the uvomorulin-catenin complex. J Cell Biol 116:989–996.

Ozawa M, Kemler R. 1998. Altered cell adhesion activity by pervanadate due to the dissociation of alpha-catenin from the E-cadherin-catenin complex. J Biol Chem 273:6166–6170.

Provost E, Rimm DL. 1999. Controversies at the cytoplasmic face of the cadherin-based adhesion complex. Curr Opin Cell Biol 11:567–572.

Qian X, Karpova T, Sheppard AM, McNally J, Lowy DR. 2004. E-cadherin mediated adhesion inhibits ligand-dependent activation of diverse receptor tyrosine kinases. EMBO J 23:1739–1748.

Rimm DL, Morpanels JS. 1994. Molecular cloning of human E-cadherin suggests a novel subdivision of the cadherin superfamily. Biochem Biophys Res Commum 200:1754–1761.

Roberts PC, Garten W, Klenk HD. 1993. Role of conserved glycosylation sites in maturation and transport of influenza A virus hemagglutinin. J Virol 67:3048–3060.

Rudd PM, Dwek RA. 1997. Glycosylation: Heterogeneity and the 3D structure of proteins. Crit Rev Biochem Mol Biol 32:1–100.

Serres M, Filhol O, Lickert H. 2000. The disruption of adherens junctions is associated with a decrease of E-cadherin phosphorylation by protein kinase CK2. Exp Cell Res 257:255–264.

Tunggal JA, Helfrich I, Schmitz A, Schwarz H, Gunzel D, Fromm M, Kemler R, Krieg T, Niessen CM. 2005. E-cadherin is essential for in vivo epidermal barrier function by regulating tight junctions. EMBO J 24: 1146–1156.

Wu GC, Lai HL, Lin YW, Chu YT, Chern Y. 2001. N-glycosylation and residues Asn805 and Asn890 are involved in the functional properties of type VI adenylyl cyclase. J Biol Chem 276:35450–35457.

Xia BY, Royall JA, Damera G, Sachdev GP, Cummings RD. 2005. Altered O-glycosylation and sulfation of airway mucins associated with cystic fibrosis. Glycobiology 15: 747–775.

Yoshimura M, Ihara Y, Matsuzawa Y, Taniguchi N. 1996. Aberrant glycosylation of E-cadherin enhances cell-cell binding to suppress metastasis. J Biol Chem 271:13811–13815.

Zhong X, Malhotra R, Woodruff R, Guidotti G. 2001. Mammalian plasma membrane ecto-nucleoside triphosphate diphosphohydrolase 1, CD39, is not active intracellularly. The N-glycosylation state of CD39 correlates with surface activity and localization. J Biol Chem 276: 41518–41525.

Zhurinsky J, Shtutman M, Ben-Ze'ev A. 2000. Plakoglobin and beta-catenin: Protein interactions, regulation and biological roles. J Cell Sci 113:3127–3139.